

## Recent Experimental Advances on Excited-State Intramolecular Proton Coupled Electron Transfer Reaction

CHENG-CHIH HSIEH, CHANG-MING JIANG, AND PI-TAI CHOU\*

*Department of Chemistry, National Taiwan University, Taipei, 106,  
Taiwan, Republic of China*

RECEIVED ON APRIL 8, 2010

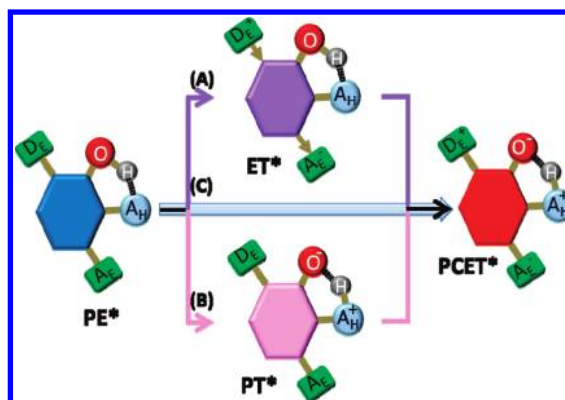
### CON SPECTUS

Proton-coupled electron transfer reactions form the basis of many important chemical processes including much of the energy conversion that occurs within living cells. However, much of the physical chemistry that underlies these reaction mechanisms remains poorly understood.

In this Account, we report on recent progress in the understanding of excited-state intramolecular proton-coupled electron transfer (PCET) reactions. The strategic design and synthesis of various types of PCET molecules, along with steady-state and femtosecond time-resolved spectroscopy, have uncovered the mechanisms of several excited-state PCET reactions in solution. These experimental advancements correlate well with current theoretical models, in which the proton has quantum motion with a high probability of tunneling. In addition, the rate of proton transfer is commonly incorporated within the rate of rearrangement of solvent molecules. As a result, the reaction activation free energy is essentially governed by the solvent reorganization because the charge redistribution is considered based on a solvent polarity-induced barrier instead of the height of the proton migration barrier.

In accord with this theoretical basis, we can rationalize the observation that the proton transfer for many excited-state PCET systems occurs during the solvent relaxation time scale of 1–10 ps: the highly exergonic reaction takes place before the system reaches its equilibrium polarization. Also, we have used various derivatives of proton transfer molecules, especially those of 3-hydroxyflavone to clearly demonstrate how researchers can tune the dynamics of excited-state PCET through changes in the magnitude or direction of the dipole vector within the reaction. Subsequently, using 2-(2'-hydroxyphenyl)-benzoxazole as the parent model, we then report on methods for the development of an ideal system for probing PCET reaction.

Because future biomedical applications of such systems will likely occur in aqueous environments, we discuss various 7-azaindole analogues, for which proton transfer requires the assistance of protic solvent molecules. These results provide a unique contrast to the ubiquitous studies on the dynamic solvent effects of PCET molecules that undergo intrinsic intramolecular proton motion.



### 1. Introduction

From the viewpoint of physical chemistry, one important as well as fundamental issue of current interest is the proton-coupled electron transfer (PCET) reaction in solution.<sup>1–3</sup> Of special interest are those associated with electronically excited-

state intramolecular PCET, for which the reaction could be triggered by photoexcitation and subsequently resolved via the corresponding relaxation dynamics. From the experimental point of view, on the one hand, the obstacle lies in the fact that strategic design of excited-state intramolecular

PCET molecules is a nontrivial task. On the other hand, except for rather simple systems, the theoretical approach on proton migration associated with great charge redistribution in the electronically excited state is still formidable. Suffice it to say that the solvent dynamics play a pivotal role in excited-state PCET reactions in solution.

In this Account, first, we briefly review current theoretical advances regarding PCET. Subsequently, to give the reader an intuitive design strategy, we then distinguish the chromophores incorporated in PCET systems according to their design, namely, excited-state intramolecular proton transfer (ESIPT) and excited-state intramolecular electron transfer (ESIET). We then demonstrate that the results of experimental advancement correlate well with contemporary theoretical models. In view of future biological applications, additional attention is also paid to the excited-state PCET reaction dynamics in alcohol and aqueous solutions. In this approach, PCET systems stemming from various 7-azaindole (7AI) analogues in protic solvents are discussed. 7AI possesses a sterically hindered four-membered-ring hydrogen bond and requires guest molecules such as protic solvent molecules to assist proton transfer in the excited state. This provides a unique case in stark contrast to the ubiquitous proton transfer systems.

## 2. Fundamental Background

Seminal and elegant theoretical approaches for ground-state PCET reaction in solution have revealed several key features in describing dynamics and electronic structures during the proton motion. One of the modern aspects is that proton motion is treated in a quantum, rather than in the classical, manner. Additionally, the motion is commonly incorporated with the rearrangement of solvent molecules. These theoretical advancements have incorporated both solvent reorganization and proton tunneling and made the framework similar to that of electron transfer reaction. Depending on degrees of coupling between reactant and product potential energy surfaces, the overall proton transfer process can thus be categorized into two regimes similar to the classifications in electron transfer reaction, namely, nonadiabatic<sup>4</sup> and adiabatic<sup>5</sup> limits. In the nonadiabatic regime, which corresponds to weak hydrogen-bonding, the rate constant of proton transfer,  $k_{PT}$ , is expressed as

$$k_{PT} = \frac{C^2}{\hbar} \sqrt{\frac{\pi}{E_s RT}} \exp\left(-\frac{\Delta G^\ddagger}{RT}\right) \quad (1)$$

$$\Delta G^\ddagger = \frac{(\Delta G + E_s)^2}{4E_s} \quad (2)$$

where  $\Delta G$  and  $\Delta G^\ddagger$  denote the reaction free energy and reaction barrier, respectively (Figure 1),  $E_s$  is the solvent reorganization energy, and  $C$  represents the proton coupling's quantum average over the vibrational modes associated with the proton motion.

Alternatively, when the hydrogen bonding strength is large, the coupling between reactant and product states becomes apparent. Similar to the electron transfer case, this situation is classified into the adiabatic regime. The proton transfer rate constant is

$$k_{PT} \equiv \frac{\omega_s}{2\pi} \exp\left(\frac{-\Delta G_{ad}^\ddagger}{RT}\right) \quad (3)$$

where  $\omega_s$  stands for solvent fluctuation frequency in the reactant well, and  $\Delta G_{ad}^\ddagger$  denotes the adiabatic reaction activation barrier.

To which category the proton-transfer reaction is favorably ascribed depends on coupling between reactant and product electronic states, which is rather sensitive to the distance between proton donor and acceptor, or in other words, hydrogen bonding strength. The larger electronic coupling not only reduces the barrier height but also narrows the width. As derived above, the reaction activation free energy ( $\Delta G^\ddagger$ , eq 1) for the proton transfer reaction is thus essentially correlated with the solvent reorganization energy ( $E_s$ ), rather than being given by the height of proton migration intrinsic barrier ( $E_i$  in Figure 1). Clearly, the solvent coordinate, instead of the proton coordinate, serves as the reaction coordinate within the proton transfer process. Since the approximation adopts the free energy along the solvent coordinate by a simple para-

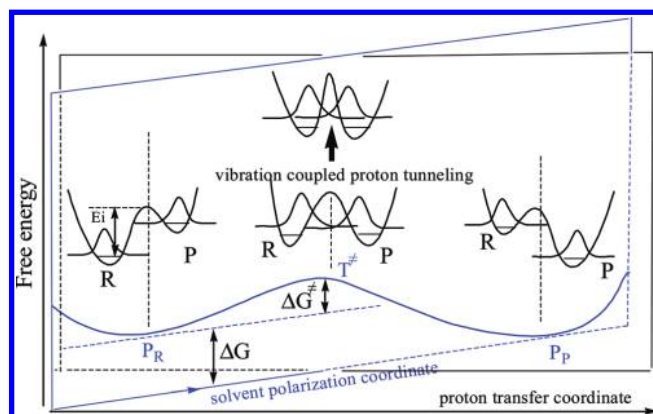


**FIGURE 1.** Free energy curves vs proton transfer at the reactant  $P_R$ , transient state,  $T^\ddagger$ , and product state,  $P_P$ , solvent polarization coordinate. The diabatic proton vibrational energy levels of each solvent polarization configuration are indicated for both the reactant and product proton wells.

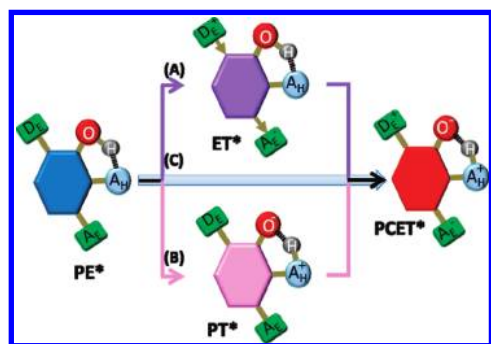


**FIGURE 2.** A generalized ESIE/ESIPT system and its possible reaction patterns.

bolic function, the amplitude of reaction activation energy can thus be analytically determined by three factors: (i) reaction thermodynamics (vertical displacement), (ii) dipole moment difference between normal and tautomer forms (horizontal displacement), and (iii) solvent polarity (curvature). The influence of each case will be discussed according to the various strategic designs of PCET molecules elaborated in the following sections.

### 3. Contemporary Experimental Advances on PCET Reaction

Experimentally, to probe the solvent polarity effect, it is crucial to fully comprehend the occurrence of ESIPT accompanied by large changes of dipole moment, such that a proton transfer event could be greatly sensitive to the solvent polarity effect.<sup>6–10</sup> Also, to avoid bimolecular complexity, especially those reaction rates determined by the diffusion limit, a unimolecular system, that is, a system invoking the excited-state intramolecular rather than intermolecular proton transfer, has received particular attention. Moreover, to anticipate a great change in dipole moment sensitive enough to probe solvent dynamics amid ESIPT, prototypical PCET systems are strategically designed to incorporate both ESIPT and ESIE properties. A conceptual ESIPT/ESIE coupled system is generalized and depicted in Figure 2, wherein  $D_E$  and  $A_E$  denote the electron donor and acceptor, respectively. In most cases,  $D_E$  and  $A_E$  are separated by a chromophore (represented by an aromatic-like structure), and their relative positions may be suitable for charge transfer reactions via, for example,  $\pi$  electron delocalization in the excited state. In most designed systems, a hydroxyl or amino hydrogen forms an intramolecular hydrogen bond with a proton acceptor ( $A_H$ ) such as azo and carbonyl groups.<sup>6–10</sup> Overall, this coupled proton/electron transfer system is denoted as PE. On the one hand, electronically exciting PE to PE\* may cause charge transfer, forming a charge transfer species ET\* (Figure 2A). On the other hand, the

hydrogen-bonded H atom may act as a strong photoacid, such that proton transfer takes place upon excitation, resulting in a proton transfer tautomer denoted by PT\* (Figure 2B). Depending on the reaction time domain, studies of ESIE vs ESIPT can be classified into two categories: (A) When the rate of ESIE is faster than that of ESIPT, following PE\* → ET\* charge transfer, the ET\* → PCET\* proton transfer reaction then takes place. (B) When ESIPT takes place prior to ESIE, the overall reaction may be described as a PE\* → PT\* proton transfer, followed by a PT\* → PCET\* charge transfer process. (C) When the electron and proton transfer simultaneously (the concerted mechanism), the reaction may be described as PE\* → PCET\* (Figure 2C). It should be noted that Hynes' formulation only considers pure proton migration and is not sufficient to describe the last case. Hammes-Schiffer and co-workers have extended Hynes' work and established a theoretical PCET model consisting of one set of four diabatic states corresponding to different ET and PT statuses.<sup>3</sup> For a fixed proton-donor-acceptor distance  $R$ , the rate constant in the nonadiabatic regime is expressed as

$$k = \sum_{\mu} P_{\mu} \sum_{\nu} \frac{|V_{\mu\nu}|^2}{\hbar} \sqrt{\frac{\pi}{\lambda_{\mu\nu} k_B T}} \exp\left[-\frac{(\Delta G_{\mu\nu} + \lambda_{\mu\nu})^2}{4\lambda_{\mu\nu} k_B T}\right] \quad (4)$$

where the summations are over reactant (PE\*) and product (PCET\*) vibronic states,  $P_{\mu}$  is the Boltzmann probability for the reactant state  $\mu$ ,  $V_{\mu\nu}$  is the vibronic coupling between the reactant and product vibronic states  $\mu$  and  $\nu$ ,  $\lambda_{\mu\nu}$  is the solvent reorganization energy for states  $\mu$  and  $\nu$ , and  $\Delta G_{\mu\nu}$  is the free energy of reaction for states  $\mu$  and  $\nu$ . Accordingly, whether the PCET is sequential or concerted depends on the relative free energy of these four diabatic states, as well as couplings between them. This model, especially the part focusing on concerted PCET, is more relevant as a theoretical basis of, for example, case C.

Based on the above concept, a number of potential PCET systems have been synthesized and investigated. Figure 3 depicts three prototypes of interest: 4'-*N,N*-diethylamino-3-hydroxyflavone (**1**),<sup>8–10</sup> 2-hydroxy-4-(di-*p*-tolylamino)benzaldehyde (**1a**),<sup>6</sup> and 2-(2'-hydroxy-4'-diethylaminophenyl)benzothiazole (**1b**),<sup>7</sup> which are developed on the basis of their parent ESIPT molecules 3-hydroxyflavone (3HF),<sup>11</sup> 2-hydroxybenzaldehyde,<sup>12</sup> and 2-(2'-hydroxyphenyl)benzothiazole,<sup>13</sup> respectively. In this approach, the *N,N*-dialkyl or -diphenyl amino groups are strategically designed to act as an electron donor, while the carbonyl oxygen or the nitrogen group within the parent ESIPT moiety serves as an electron acceptor (Figure 3).

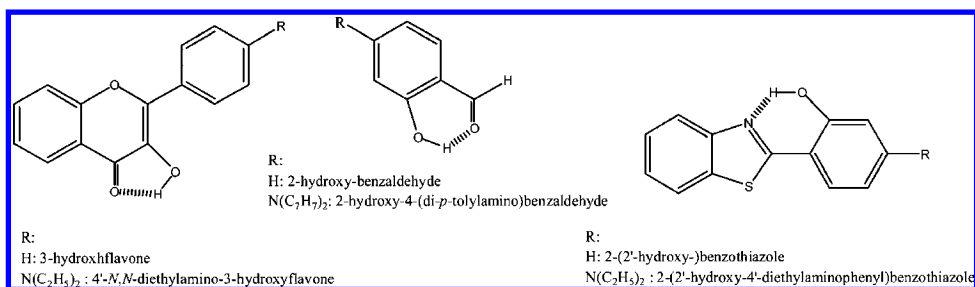


FIGURE 3. Molecular structures of some representative PCET systems and their parent ESIPT molecules.

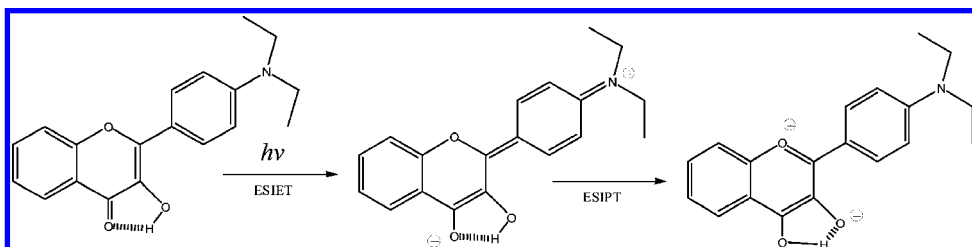


FIGURE 4. Using compound **I** as a paradigm to demonstrate the “case A” PCET model.

Up to this stage, the experimental data collected<sup>6–10</sup> have drawn the conclusion that most PCET systems designed above (Figure 3) can be ascribed to case A (Figure 2), for which an ultrafast ESIET (much less than the system response of 150 fs) takes place prior to ESIPT. Using compound **I** as a paradigm, a PCET route is delineated in Figure 4 to manifest the “case A” model. The results may not be too surprising, for they can be rationalized by a strong  $\pi$ -orbital overlap between electron donor and acceptor moieties for the designed systems, such that the electronic coupling matrix is  $\gg k_B T$  ( $\sim 200$  cm<sup>-1</sup> at 298 K), being much larger than that of the Marcus type of weak-coupling electron transfer.<sup>14</sup> The ESIET for **I**, and likewise for **Ia** and **Ib**, can thus be considered as an adiabatic electron transfer process or even an optical electron transfer<sup>14</sup> that occurs during the Franck–Condon excitation.

Despite its straightforward depiction, however, Figure 4 oversimplifies the PCET mechanism. Detailed femtosecond fluorescence up-conversion studies, particularly on the rise dynamics of the proton transfer tautomer emission, have revealed a new insight, that there always exists a fast rise component (on the order of system response limits of 150 fs to several picoseconds) on the proton transfer tautomer emission, the rate of which seems to correlate with solvent relaxation dynamics monitored at the electron transfer emission band. In other words, in these systems (**I**, **Ia**, and **Ib**), after optical ESIET, it is found that ESIPT, as monitored by the appearance of the proton transfer tautomer, always takes place prior to the reaching of solvent equilibration; its rate is complicated by the competitive solvent relaxation process, that is, the  $ET^* \rightarrow ET_{eq}^*$  process (the subscript “eq” denotes the solvent equilibrated state; see Figure 5). This phenomenon has been pre-

viously unrecognized<sup>8–10</sup> and is of fundamental importance. The results can be rationalized by highly exergonic reaction for ESIPT upon Franck–Condon excitation. Such ESIPT reaction proceeds via a fast tunneling process, the rate of which is competitive with the solvent relaxation process. Thus, the relaxation time scale of the solvent should play a role in the early relaxation dynamics. In the nonequilibrium region of the  $ET^*$  state, the solvent relaxation time scale competes with the ESIPT reaction for all cases applied here. Accordingly, the fast decay time of, for example, normal emission is dominated by ESIPT incorporated with solvent relaxation dynamics. After proton transfer in the nonequilibrium region, the resulting vibrationally hot, nonequilibrated tautomer species then undergo internal conversion or solvent relaxation to reach the equilibrium polarization. The result manifests the importance of driving force harnessed by reaction thermodynamics, that is, the (i) vertical displacement elaborated in section 2.

After reaching the solvent equilibration for  $ET^*$ , then due to the difference in equilibrium polarization between  $ET_{eq}^*$  and  $PCET_{eq}^*$ ,  $ET_{eq}^* \rightarrow PCET_{eq}^*$  proton transfer reaction is associated with an appreciable solvent-induced barrier, as evidenced by the much slower  $ET_{eq}^* \rightarrow PCET_{eq}^*$  rate of several tens of picoseconds, which is in sharp contrast to the rate of  $\gg 10^{12}$  s<sup>-1</sup> ( $\tau_f \ll 1$  ps) for those ESIPT systems having negligible changes in dipole moment during the reaction.<sup>6–10</sup> Consequently, the results, reflected by the steady-state approach, commonly show dual emission consisting of  $ET_{eq}^*$  and  $PCET_{eq}^*$  emission (Figure 6). Since the reaction barrier is introduced by the difference in solvent polarity function between reactant  $ET_{eq}^*$  and product  $PCET_{eq}^*$ , the system provides a unique case in point of utilizing proton transfer reaction rather than the electron trans-

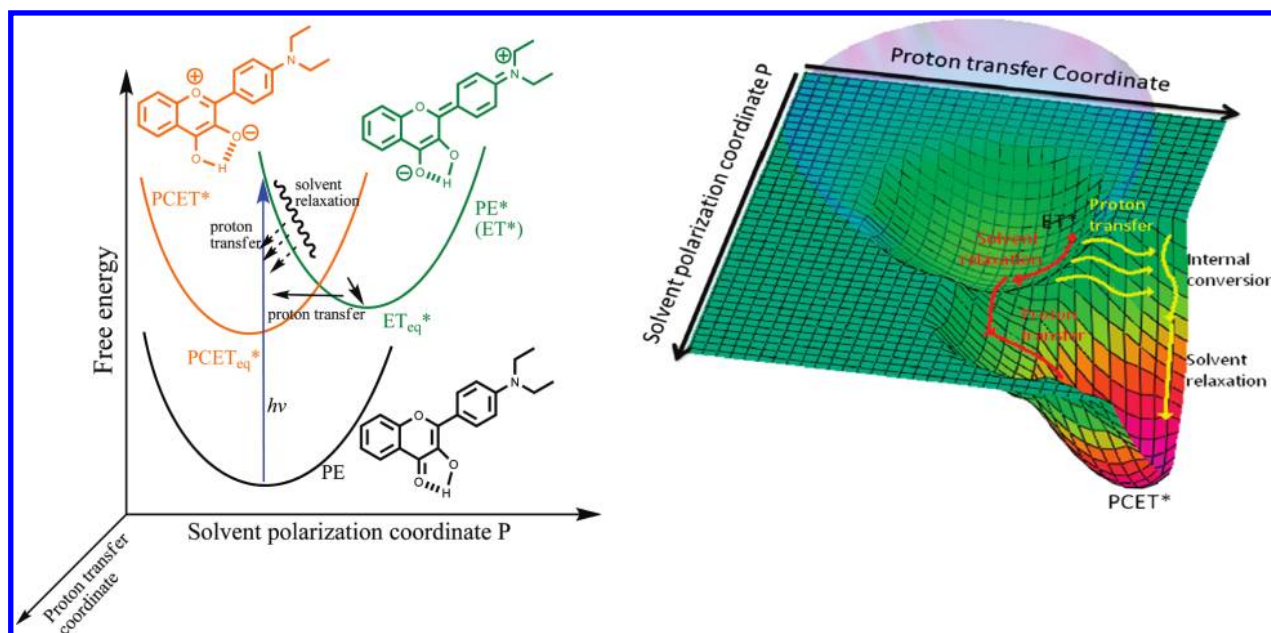


FIGURE 5. (left) Relaxation processes for case A PCET system using compound **I** as an example and (right) a 3-D depiction.

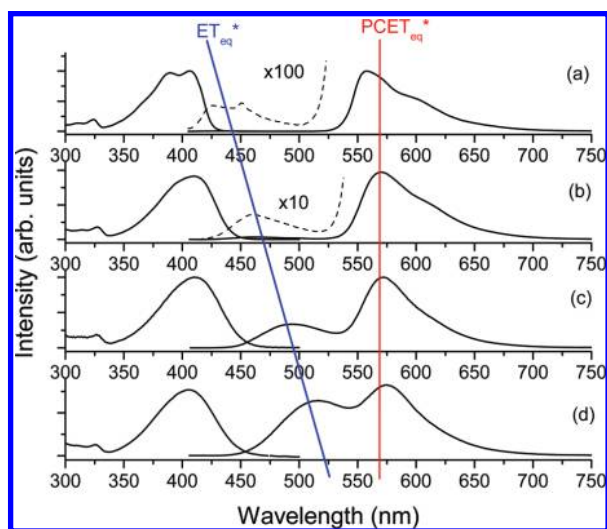


FIGURE 6. Static absorption and fluorescence spectra of **I** in (a) cyclohexane, (b) benzene, (c) dichloromethane, and (d) acetonitrile at 298 K.<sup>10</sup>

fer to probe whether the barrier, that is, the proton transfer rate, is solvent polarity dependent. In other words, the system is ideal to test the influence of proton transfer rate by reaction thermodynamics, namely, the aforementioned (i) vertical displacement and (iii) solvent polarity.

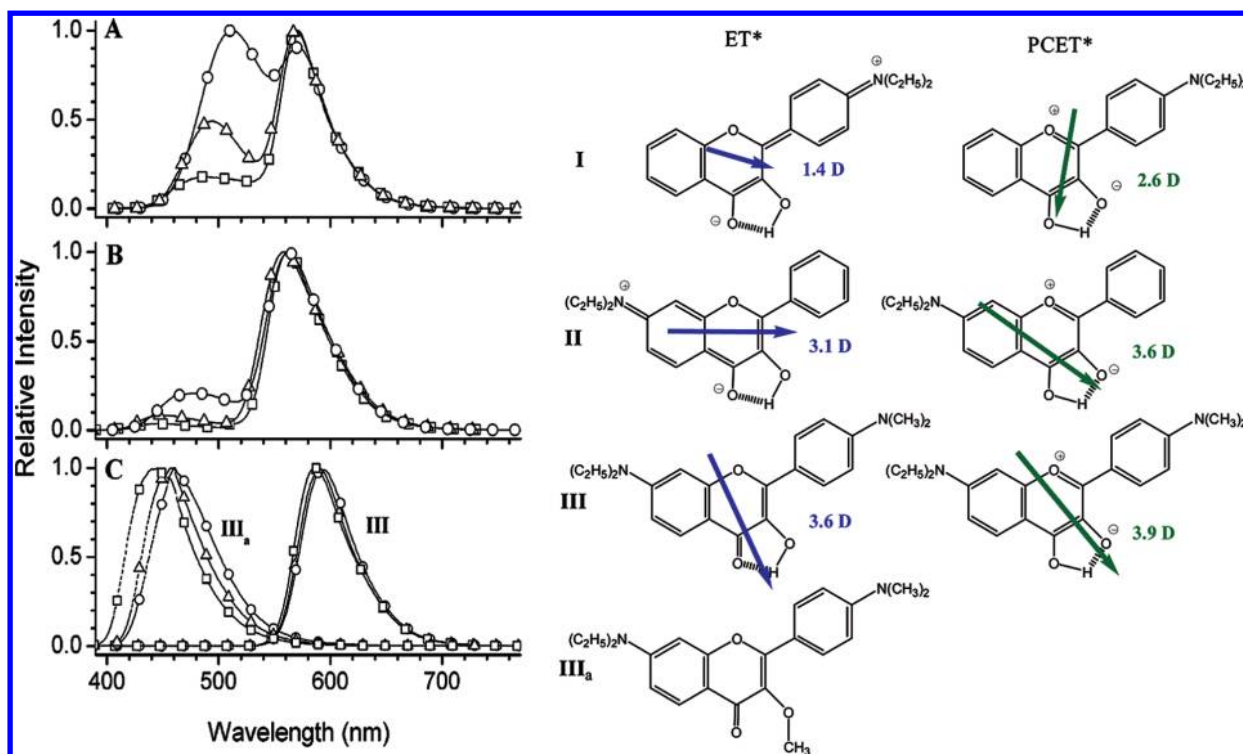
The result for **I** shown in Table 1 clearly demonstrates that the rate of  $ET_{eq}^* \rightarrow PCET_{eq}^*$  proton transfer decreases upon increasing the solvent polarity from cyclohexane, (2 ps)<sup>-1</sup>, to acetonitrile, (30 ps)<sup>-1</sup>. Despite the solvent polarity dependence, the result seems to be the reverse of that predicted by electron transfer theory: it is faster in the more polar solvent. At first glance, the observations may be consistent with larger reorganization energy and hence a slower proton transfer rate

TABLE 1. Summary of Photophysical Properties of **I** in Various Solvents

solvent	emission	early dynamics/ps	population decay/ns
cyclohexane	ET*, 425 nm PCET*, 560 nm	decay, 2.1 rise, 2.0	1.28 (for PCET* only)
benzene	ET*, 460 nm PCET*, 570 nm	decay, 9.9 rise, 10.0	0.9 (for PCET* only)
CH <sub>2</sub> Cl <sub>2</sub>	ET*, 495 nm PCET*, 570 nm	decay, 34.7 rise, 25.0	0.72
CH <sub>3</sub> CN	ET*, 510 nm PCET*, 575 nm	decay, 30.8 rise, 23.4	0.43

in a more polar solvent, assuming that the reorganization energy for proton transfer is much smaller than that for electron transfer. Alternatively, as also supported by case B systems (vide infra), the result can be unambiguously rationalized by the reactant  $ET_{eq}^*$  having a larger dipole moment vector (in magnitude) due to its charge transfer character than that of the product  $PCET_{eq}^*$ . As a result, the reactant  $ET_{eq}^*$  is more stabilized with increased solvent polarity (Figure 5, left). In contrast, electron transfer in many cases proceeds from neutral to charged species, such that the product, or the charged species, is stabilized by polar solvents. Moreover, all systems **I**, **Ia**, and **Ib** have similar trends of solvent-polarity dependent reaction dynamics, indicating that the designed systems can be ascribed to the *normal region* if Marcus electron transfer theory is adopted.

From the chemistry point of view, one intriguing issue relevant to the above approach may lie in the fact that the degree of changes in terms of either magnitude or orientation of dipole moment for ESIET, and hence the following



**FIGURE 7.** Molecular structures and the emission spectra of (A) **I**, (B) **II**, and (C) **III** (solid line) and **III<sub>a</sub>** (dash line) in ethyl acetate ( $\square$ ),  $\text{CH}_2\text{Cl}_2$  ( $\Delta$ ), and  $\text{CH}_3\text{CN}$  ( $\circ$ ) and the calculated dipole moments for **I**, **II** and **III** in  $\text{ET}^*$  and  $\text{PCET}^*$  state.<sup>9</sup>

ESIPT, as well as overall PCET reaction dynamics, can be fine-tuned via chemical modification. Recently, proof of this concept has been demonstrated by employing three analogues of 3-hydroxyflavone, namely, compound **I**, 7-*N,N*-diethylamino-3-hydroxyflavone (**II**), and 4'-*N,N*-dimethylamino-7-*N,N*-diethylamino-3-hydroxyflavone (**III**), shown in Figure 7. Upon substitution of the electron-accepting dialkylamino moiety at different positions or in opposite directions for dipole cancellation, an ingenious approach to fine-tuning the PCET reaction via the molecular framework can be achieved.<sup>9</sup> Due to the great difference in dipole vector between  $\text{ET}^*$  and  $\text{PCET}^*$  states, and hence the large solvent-polarity induced barrier, both **I** and **II** exhibit remarkable dual emission. Conversely, the dipole cancellation of two charge-transfer entities in **III** leads to ESIPT being decoupled from the solvent-polarity effect, resulting in a unique, solvent polarity independent proton-transfer tautomer emission (Figure 7). The results make feasible further rational design and systematic investigation of PCET systems fine-tuned by the net dipolar effect.

The experimental progress elaborated above is of great fundamental importance in that it clearly addresses the role of solvent polarity channeling into the proton-transfer dynamics. Unfortunately, up to this stage, for most experimental model systems applied, the PCET dynamics are ascribed to case A, in which ESIET takes place prior to ESIPT. Thus, the Franck–Condon excitation generates a nonequilibrium  $\text{ET}^*$

state. Subsequently, the associated proton transfer dynamics to be probed are complicated by the competitive solvent relaxation and perhaps highly exergonic ESIPT prior to reaching the equilibrium polarization (vide supra). Thus, studies of PCET reaction dynamics commonly encounter interference by the rate of solvent relaxation. To circumvent this hurdle, it should be a matter of great fundamental interest, as well as of urgency, to look for an ideal PCET system free from the interference of early solvent relaxation. In theory, a case in point stems from case B (Figure 2), for which the molecule designated should meet the prerequisite that it undergoes ESIPT prior to the ESIET reaction. Moreover, if the system is designed such that the electron donor and acceptor are strongly  $\pi$ -conjugated with a large electronic coupling matrix, the electron transfer may simply involve instant electron relocalization. Accordingly, the overall PCET reaction can be treated as if the proton transfer took place simultaneously with the electron transfer.

The study of ESIPT-coupled ESIET, or process B, has recently become feasible via the strategic design and synthesis of the molecule 2-((2-(2-hydroxyphenyl)benzo[*d*]oxazol-6-yl)methylene)malononitrile (diCN-HBO).<sup>15</sup> From the viewpoint of molecular structure, the lone pair of electrons of the benzo-nitrogen atom in diCN-HBO are intrinsically involved in the  $\pi$ -electron resonance, that is, to establish the aromaticity, such that its electron-donating strength is much weaker compared with

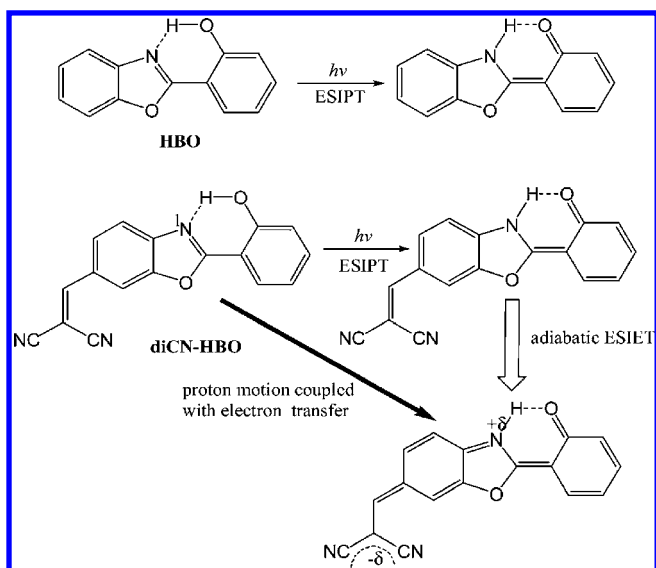


**FIGURE 8.** Proposed ES IPT reaction for HBO and PCET reaction for diCN-HBO.<sup>17</sup>

those of alkyl and aryl amines. Upon Franck–Condon excitation of diCN-HBO, the degree of charge transfer should thus be negligible. On the other hand, similar to its parent molecule 2-(2'-hydroxyphenyl)benzoxazole (HBO),<sup>16</sup> ES IPT is expected to take place from the hydroxyl proton to the N1 nitrogen (Figure 8), resulting in a proton transfer tautomer; essentially, a keto isomer. Once the proton-transfer tautomer is formed, the N1 nitrogen atom becomes the secondary alkyl amino nitrogen and thus should act as a good electron donor.

As a result, unlike most PCET systems designed above (case A), wherein ES IET takes place prior to ES IPT, diCN-HBO undergoes ES IPT, concomitantly accompanied by the charge transfer process, such that the ES IPT reaction dynamics are directly coupled with solvent polarization effects. The long-range solvent polarization interactions result in a solvent-induced barrier that affects the overall proton transfer reaction rate. Dual emission has thus been observed in diCN-HBO; the proton-transfer tautomer emission peak red shifts drastically with increased solvent polarities, while the normal emission is solvent polarity independent. This is in stark contrast to the case A systems, for which the peak wavelength of the proton-transfer (electron-transfer) emission is solvent polarity independent (dependent). In cyclohexane, the rate constant of ES IPT of diCN-HBO was determined to be  $(1.1 \text{ ps})^{-1}$ , which is apparently slower than the  $\sim(150 \text{ fs})^{-1}$  for the parent molecule HBO.<sup>16</sup> Upon an increase in the solvent polarity, the ES IPT time constants were also determined to be  $1.00 \pm 0.13 \text{ ps}$  in benzene,  $0.60 \pm 0.05 \text{ ps}$  in  $\text{CH}_2\text{Cl}_2$ , and  $0.31 \pm 0.03 \text{ ps}$  in  $\text{CH}_3\text{CN}$ , values that reveal that increasing the solvent polarity tends to render an increase in the rate of ES IPT (Figure 9).<sup>17</sup> The overall reaction dynamics can be described by a mecha-

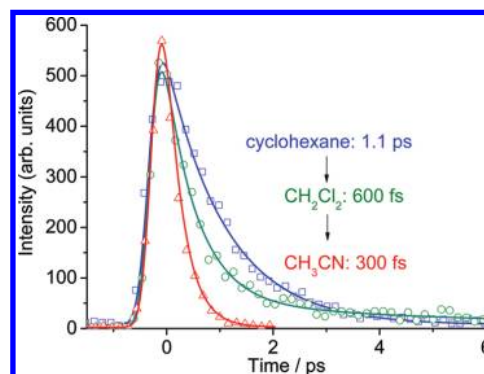


**FIGURE 9.** Time-resolved fluorescence decay of diCN-HBO in various solvents monitored at the normal emission ( $\text{PE}^*$ ).

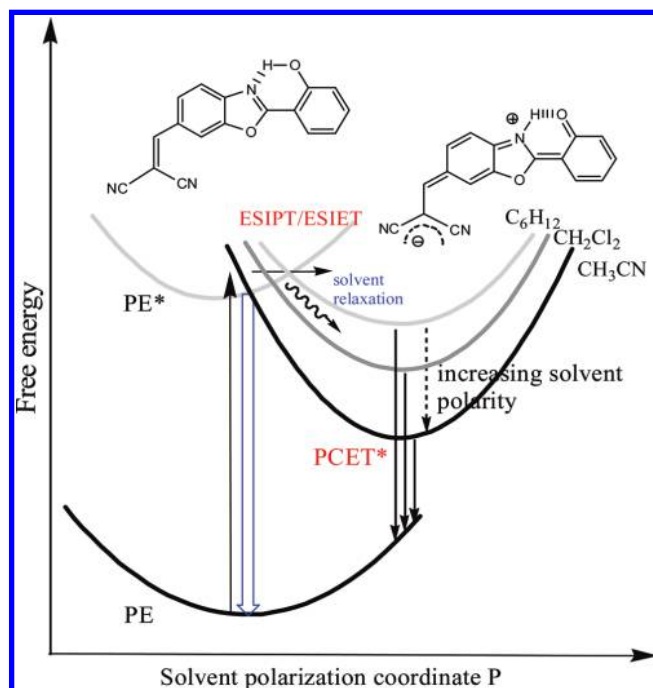


**FIGURE 10.** The proposed ES IPT/ES IET reaction and the corresponding relaxation dynamics using diCN-HBO as a model.<sup>17</sup>

nism incorporating both solvent polarization and proton-transfer reaction coordinates (Figure 10). The proton-transfer tautomer, possessing large degrees of charge-transfer character, is obviously stabilized upon increasing solvent polarity, while the influence of solvent polarity on the  $\text{PE}^*$  state is relatively much smaller; thus the corresponding solvent-induced barrier is reduced. Thus, although systems A and B (or C) show opposite trends on the solvent polarity dependent reaction rate, the results can be clearly rationalized by the fact that the polar solvent stabilizes the reactant (charged species) more than the product (neutral species) in system A while it stabilizes the product (charged species) more than the reactant (neutral species) in system B (or C).

It is also worthy of note that unlike the parent ES IPT molecule HBO, which executes ultrafast ( $<150 \text{ fs}$ ) ES IPT in non-

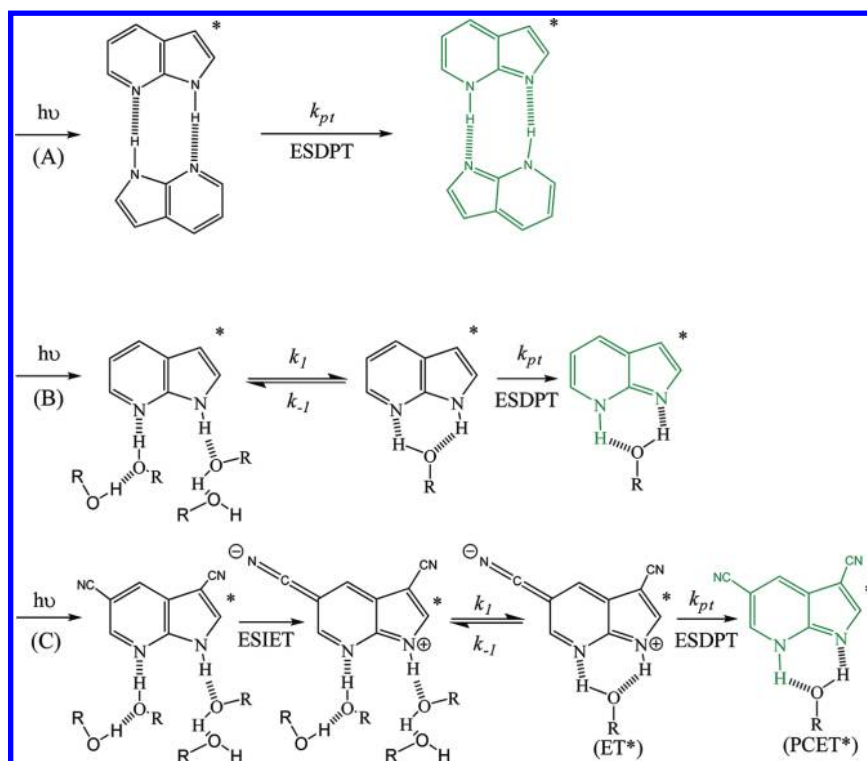


**FIGURE 11.** (A) The ESDPT of 7AI through self-dimerization,<sup>23,24</sup> (B) the ESDPT of 7AI through the assistance of solvent molecule (R = H or alkyl groups),<sup>25,28</sup> and (C) the proposed mechanism of PCET reaction of 3,5CNAI in protic solvents.

polar solvent such as cyclohexane,<sup>16</sup> the ESIP/ESIET coupled system diCN-HBO undergoes a finite time constant (1.1 ps) proton transfer in the same solvent. The result, on the one hand, can be rationalized by the non-negligible quadrupole moment effect from cyclohexane,<sup>18</sup> which induces the small solvent-perturbed barrier. On the other hand, a dynamic polarization model in nonpolar solvents has been proposed by Hamaguchi and co-workers.<sup>19</sup> Because of the appreciable dipolar change between PE\* and PCET\* in the case of diCN-HBO, the induced dipole/dipole interaction is considered to be non-negligible, inducing an appreciable barrier in the PCET reaction.

Also, recent advances in PCET systems such as O–H deuterated **I**, **II**, and diCN-HBO all showed lack of a deuterium isotope effect for  $k_{PT}$  in, for example, acetonitrile at room temperature.<sup>20</sup> As for the nonadiabatic proton transfer shown in eq 1, the pre-exponential factor that involves tunneling probability should be sensitive to the deuterium isotope substitution and accordingly affect  $k_{PT}$ . On the one hand, the lack of deuterium isotope effect on proton transfer rate may imply a rather small or even negligible barrier. This viewpoint is consistent with the ultrafast, barrierless ESIP/ESIET for their parent molecules such as 3HF<sup>11</sup> and HBO.<sup>16</sup> On the other hand, at this stage, we cannot eliminate the possibility that the reaction is an adiabatic type and that the deuterium isotope effect is too

small to be resolved with our current system. Future exploration focusing on the PCET systems in nonadiabatic regime should be of great interest. This may require the design of PCET systems with an intrinsic weak intramolecular hydrogen bond. A case in point is the 2-pyridyl pyrazole system.<sup>21</sup> Another approach for the future is to probe PCET reaction in nonpolar solvent, where the quadrupole or even octupolar (e.g., in benzene) moment effect plays a key role. This may require molecules that undergo gigantic changes of dipole moment (in either magnitude or orientation) during PCET. The design could strategically incorporate an ideally opposite dipole orientation between PE\* and PT\*.

The above approach is mainly applied in polar, aprotic solvents. As for a protic solvent to mimic the bioenvironment, the solvent hydrogen-bonding perturbation commonly leads to the rupture of solute intramolecular hydrogen bonds and hence makes such studies extremely complicated.<sup>22</sup> To probe PCET reaction in protic solvents, one has to utilize solvent molecules as a positive gain, not the interference factors for proton transfer. In other words, an ingenious thought may be that the designed system intrinsically lacks intramolecular hydrogen bonds, and ESIP/ESIET, if there is any, ought to take place via the assistance of protic solvent molecules. Under this criterion, a case in point is the 7AI type of excited-state proton-transfer systems (Figure 11A).



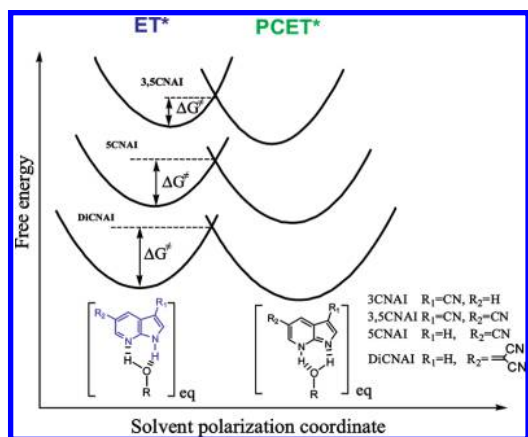


**FIGURE 12.** Following ESIT and solvent relaxation, a mechanism of proton transfer from  $ET^*$  to  $PCET^*$  incorporating solvent polarity induced barrier ( $\Delta G^\ddagger$ ) for 7AI analogues is depicted, in which the increase of dipolar separation between  $ET_{eq}^*$  and  $PCET_{eq}^*$  results in the increase of the solvent-induced barrier.<sup>27</sup>

Due to the steric hindrance of the formation of a four-membered ring intramolecular hydrogen bond, 7AI undergoes excited-state proton transfer through either self-dimerization<sup>23,24</sup> or the assistance of solvent molecules<sup>25</sup> depicted in Figure 11A,B. Both processes involve the switch of two protons and thus are excited-state double proton transfer (ESDPT) reactions. Strategically, the electron donor/acceptor functionality can be incorporated into 7AI, so that charge transfer influencing ESIT can be examined in protic solvents. Prototypes of those designated 7AI analogues, such as 5-cyano-7-azaindole (5CNAI), 3-cyano-7-azaindole (3CNAI),<sup>26</sup> 3,5-dicyano-7-azaindole (3,5CNAI), and dicyanoethenyl-7-azaindole (DiCNAI), have been designed, and their structures are depicted in Figure 12.<sup>27</sup> In this approach, on the one hand, the cyano moiety serves as an electron-withdrawing group, such that ESIT may take place from pyrrolic nitrogen to the cyano substituent. On the other hand, the pyrrolic hydrogen and the pyridinyl nitrogen act as proton donating and accepting groups, respectively, with a lack of intramolecular hydrogen bonds, such that proton transfer takes place under the assistance of solvent relay (Figure 11C).

As a result, in protic solvents such as methanol, 3CNAI and 3,5CNAI, similar to 7AI, undergo methanol-catalyzed ESDPT, revealing dual ( $ET^*$  and  $PCET^*$ ) emission.<sup>27</sup> However, proton transfer is prohibited for 5CNAI and DiCNAI in methanol, as evidenced by a unique  $ET^*$  emission. The  $ET^*$  emission for all derivatives reveals a significant charge transfer property due to its prominent solvatochromism, though to different extents. The ESDPT rate, which is determined by the rise/decay of tautomer ( $PCET^*$ )/normal ( $ET^*$ ) form emission, is shown to be quite different throughout this series of 7AI derivatives (Table 2).<sup>27</sup> For example, the time constant of proton transfer in metha-

**TABLE 2.** Photophysical Properties of 7AI and Its Correlated Cyano Analogues in Methanol

	$\lambda_{em}, \text{nm}$	$\tau, \text{ns}^a$
7AI	$ET^*$ , 374	$\tau$ , 0.146
	$PCET^*$ , 503	$\tau_1$ , 0.134 (−0.44) $\tau_2$ , 0.654 (0.56)
3CNAI	$ET^*$ , 343	$\tau$ , 0.23
	$PCET^*$ , 480	$\tau_1$ , 0.24 (−0.49) $\tau_2$ , 5.88 (0.51)
3,5CNAI	$ET^*$ , 377	$\tau$ , 0.69
	$PCET^*$ , 515	$\tau_1$ , 0.71 (−0.52) $\tau_2$ , 1.13 (0.48)

<sup>a</sup> Data in parentheses are the fitted pre-exponential factors.

noI varies from as fast as 130 ps in 7AI and 240 ps in 3CNAI to as slow as 710 ps in 3,5CNAI. In 5CNAI, it is much greater than the lifetime of the  $ET^*$  state of 4.8 ns due to the lack of resolution of any proton-transfer tautomer emission.

Evidently, the widely accepted 7AI ESDPT mechanism, which involves equilibrium between free 7AI and 1:1 solvent complex,<sup>25,28</sup> cannot explain the dynamical data adequately, because the main chromophore in these compounds remains unchanged. Likewise, due to the similar chemical structures, nor can the difference in the solvent complex equilibrium constant account for the large proton rate difference. It is thus concluded that the solvent-induced barrier plays a significant role in this system. Applying the computational approach, the dipole moment differences between normal form and tautomer in the first excited-state have been calculated to follow the trend DiCNAI > 5CNAI > 3,5CNAI > 3CNAI  $\approx$  7AI. The trend of ESDPT rate is in good correlation with the proposed solvent polarity induced barrier resulting from the difference in changes of dipole moments between the equilibrium polarization of normal ( $ET_{eq}^*$ ) and tautomer species ( $PCET_{eq}^*$ ) along the solvent coordinate (Figures 12).<sup>27</sup> As shown in Figure 11C, it is obvious that the barrier is increased upon an increase in the difference in dipole moment (either magnitude or direction) between normal and tautomer forms, supporting the theoretical prediction regarding (ii) horizontal displacement of dipole separation between normal and tautomer forms along the solvent polarization coordinate, which has been described in section 2.

Another important feature is the deuterium isotope effect for these 7AI analogues. For example, the time constant of proton transfer for 3CNAI in water decreases from N–H of 910 ps to N–D of 3.50 ns,<sup>26</sup> indicating that  $k_{PT}$  is governed by a tunneling mechanism. The difference between protic solvent (e.g., methanol or water) assisted double proton transfer in 7AI analogues and the above-mentioned intramolecular proton transfer systems lies in the difference between the intermolecular hydrogen bond versus the intrinsic intramo-

lecular hydrogen bond. The former requires formation of a cyclic hydrogen bonded solvent–7Al complex (Figure 11B,C) and is expected to be weaker due to the geometry constraint. It is noteworthy that the intrinsic proton-transfer rate for cyclic hydrogen bonded water–7Al complex has been proposed to be much slower than the solvent reorganization rate.<sup>28</sup> According to the weaker hydrogen bonding strength, we assume that PCET systems are classified into the nonadiabatic regime to simplify the discussion. Thus, the associated PCET kinetics incorporating both solvent pre-equilibrium and solvent-induced barrier can be expressed by eq 5:

$$k_{\text{PCET}} = \frac{k_1}{k_{-1}} k_{\text{PT}} = e^{-\Delta G^+/(RT)} \left[ \frac{\langle C \rangle^2}{\hbar} \sqrt{\frac{\pi}{E_s RT}} e^{-\Delta G^\ddagger/(RT)} \right] = \frac{\langle C \rangle^2}{\hbar} \sqrt{\frac{\pi}{E_s RT}} e^{-(\Delta G^+ + \Delta G^\ddagger)/(RT)} \quad (5)$$

where  $\Delta G^+$  and  $\Delta G^\ddagger$  denote the free energy difference between the two hydrogen-bonded complexes that are in equilibrium and solvent-induced barrier, respectively. Evidently, the activation free energy represents not only the free energy difference between cyclic and noncyclic solvated structures (Figure 11C) but also the incorporation of the solvent induced barrier,  $\Delta G^\ddagger$ , the tendency of which, as a function of differences in dipole moment between reactant and product, is qualitatively depicted in Figure 12.

The above advancement leads to the perspective that through ingenious design, systematic investigation of the PCET reaction in aqueous solution is feasible, which may be crucial to gaining fundamental insights into the current research fields regarding, for example, PCET in a living system.

## 4. Concluding Remarks

In sum, despite the ultrafast, nearly barrierless ES IPT in gas as well as in nonpolar solvents, such that either coherent, ballistic, or hydrogen-bond associated vibrational mode induced proton transfer have been proposed for numerous molecules,<sup>29</sup> it is still true that in polar solvents, due to the common changes of dipole moment during ES IPT, the solvent polarity is expected to play a crucial role, which may channel into the reaction dynamics. Theory on solvent polarity induced proton transfer reaction dynamics has been briefly discussed, followed by the classification based on two types of designed experiments, namely, the charge transfer induced proton transfer reaction (case A) and proton transfer induced charge transfer reaction (case B). Both prove to be useful for describing excited-state intramolecular PCET reaction, for which the systems designed are ascribed to the adiabatic

regime. In another approach, PCET is also probed in protic solvents based on host/guest types of hydrogen-bonding complexes, which are classified into the nonadiabatic regime. The PCET dynamics fine-tuned by solvent polarity, as well as the differences in thermodynamics and dipole vector between reactant and product, have been discussed in a comprehensive manner. For future study, it is of fundamental interest to examine whether the dipolar tuning mechanism can be generalized to other PCET systems. For example, the design of a system exhibiting nonadiabatic type electron transfer followed by an adiabatic type proton transfer is another highlighted issue in investigating proton transfer kinetics. In this case, the reaction rate-limiting step may be determined by the electron transfer, rather than by the proton transfer process. Thus, the interplay between ES IPT reaction and the function of solvent polarity should be of great interest and importance. We thus hope this Account provides profound fundamental insight that will lead chemists to further extend PCET fundamentals and applications in greater depth and breadth.

## BIOGRAPHICAL INFORMATION

**Cheng-Chih Hsieh** is a Ph.D. student in Prof. Pi-Tai Chou's lab at NTU (2005–2010). He is currently working on ultrafast time-resolved spectroscopy.

**Chang-Ming Jiang** is a former research assistant in Prof. Pi-Tai Chou's lab at NTU (2008–2009). He is currently pursuing a Ph.D. at the University of California, Berkeley (2009–2010), where he is working in Stephen Leone's group.

**Pi-Tai Chou** received his Ph.D. degree from Florida State University, Tallahassee, in 1985 and is currently the Chairman of the Chemistry Department and a Chair Professor at National Taiwan University (NTU). Prior to joining NTU, he was a DOE postdoctoral fellow at the University of California, Berkeley (1985–1987), an assistant professor at the University of South Carolina, Columbia (1987–1994), and a professor at National Chung Cheng University (1994–2000). His research interests are in the area of ultrafast phenomena on excited-state proton/charge and energy transfer reactions and syntheses, photophysics, and applications of materials suited for OLEDs, solar energy cells, and nanotechnology.

## FOOTNOTES

\*To whom correspondence should be addressed. E-mail: chop@ntu.edu.tw.

## REFERENCES

- Cukier, R. I. A theory that connects proton-coupled electron-transfer and hydrogen-atom transfer reactions. *J. Phys. Chem. B* **2002**, *106*, 1746–1757.
- Li, B.; Zhao, J.; Onda, K.; Jordan, K. D.; Yang, J.; Petek, H. Ultrafast interfacial proton-coupled electron transfer. *Science* **2006**, *311*, 1436–1440.
- Hammes-Schiffer, S.; Soudackov, A. V. Proton-coupled electron transfer in solution, proteins, and electrochemistry. *J. Phys. Chem. B* **2008**, *112*, 14108–14123, and references therein.

- 4 Kiefer, P. M.; Hynes, J. T. Kinetic isotope effects for nonadiabatic proton transfer reactions in a polar environment. 1. Interpretation of tunneling kinetic isotope effects. *J. Phys. Chem. A* **2004**, *108*, 11793–11808.
- 5 Kiefer, P. M.; Hynes, J. T. Nonlinear free energy relations for adiabatic proton transfer reactions in a polar environment. I. Fixed proton donor-acceptor separation. *J. Phys. Chem. A* **2002**, *106*, 1834–1849.
- 6 Chou, P.-T.; Yu, W.-S.; Cheng, Y.-M.; Pu, S.-C.; Yu, Y.-C.; Lin, Y.-C.; Huang, C.-H.; Chen, C.-T. Solvent-polarity tuning excited-state charge coupled proton-transfer reaction in *p*-*N,N*-ditolylaminosalicylaldehydes. *J. Phys. Chem. A* **2004**, *108*, 6487–6498.
- 7 Cheng, Y.-M.; Pu, S.-C.; Hsu, C.-J.; Lai, C.-H.; Chou, P.-T. Femtosecond dynamics on 2-(2'-hydroxy-4'-diethylaminophenyl)benzothiazole: Solvent polarity in the excited-state proton transfer. *ChemPhysChem* **2006**, *7*, 1372–1381.
- 8 Shynkar, V. V.; Mély, Y.; Duportail, G.; Piémont, E.; Klymchenko, A. S.; Demchenko, A. P. Picosecond time-resolved fluorescence studies are consistent with reversible excited-state intramolecular proton transfer in 4'-(dialkylamino)-3-hydroxyflavones. *J. Phys. Chem. A* **2003**, *107*, 9522–9529.
- 9 Chou, P.-T.; Huang, C.-H.; Pu, S.-C.; Cheng, Y.-M.; Liu, Y.-H.; Wang, Y.; Chen, C.-T. Tuning excited-state charge/proton transfer coupled reaction via the dipolar functionality. *J. Phys. Chem. A* **2004**, *108*, 6452–6454.
- 10 Chou, P.-T.; Pu, S.-C.; Cheng, Y.-M.; Yu, W.-S.; Yu, Y.-C.; Hung, F.-T.; Hu, W.-P. Femtosecond dynamics on excited-state proton/charge-transfer reaction in 4'-*N,N*-diethylamino-3-hydroxyflavone. The role of dipolar vectors in constructing a rational mechanism. *J. Phys. Chem. A* **2005**, *109*, 3777–3787.
- 11 McMorrow, D.; Kasha, M. Intramolecular excited-state proton transfer in 3-hydroxyflavone. Hydrogen-bonding solvent perturbations. *J. Phys. Chem.* **1984**, *88*, 2235–2243.
- 12 Nagaoka, S.; Hirota, N.; Sumitani, M.; Yoshihara, K. Investigation of the dynamic processes of the excited states of *o*-hydroxybenzaldehyde and *o*-hydroxyacetophenone by emission and picosecond spectroscopy. *J. Am. Chem. Soc.* **1983**, *105*, 4220–4226.
- 13 Frey, W.; Laermer, F.; Elsaesser, T. Femtosecond studies of excited-state proton and deuterium transfer in benzothiazole compounds. *J. Phys. Chem.* **1991**, *95*, 10391–10395.
- 14 Penfield, K. W.; Miller, J. R.; Paddon-Row, M. N.; Cotsaris, E.; Oliver, A. M.; Hush, N. S. Optical and thermal electron transfer in rigid difunctional molecules of fixed distance and orientation. *J. Am. Chem. Soc.* **1987**, *109*, 5061–5065.
- 15 Seo, J.; Kim, S.; Park, S. Y. Strong solvatochromic fluorescence from the intramolecular charge-transfer state created by excited-state intramolecular proton transfer. *J. Am. Chem. Soc.* **2004**, *126*, 11154–11155.
- 16 Wang, H.; Zhang, H.; Abou-Zied, O. K.; Yu, C.; Romesberg, F. E.; Glasbeek, M. Femtosecond fluorescence upconversion studies of excited-state proton-transfer dynamics in 2-(2'-hydroxyphenyl)benzoxazole (HBO) in liquid solution and DNA. *Chem. Phys. Lett.* **2003**, *367*, 599–608.
- 17 Hsieh, C.-C.; Cheng, Y.-M.; Hsu, C.-J.; Chen, K.-Y.; Chou, P.-T. Spectroscopy and femtosecond dynamics of excited-state proton transfer induced charge transfer reaction. *J. Phys. Chem. A* **2008**, *112*, 8323–8332.
- 18 Craven, I. E.; Hesling, M. R.; Laver, D. R.; Lukins, P. B.; Ritchie, G. L. D.; Vrbancich, J. Polarizability anisotropy, magnetic anisotropy, and quadrupole moment of cyclohexane. *J. Phys. Chem.* **1989**, *93*, 627–631.
- 19 Iwata, K.; Ozawa, R.; Hamaguchi, H. Analysis of the solvent- and temperature-dependent Raman spectral changes of S1 trans-stilbene and the mechanism of the trans to cis isomerization: Dynamic polarization model of vibrational dephasing and the C=C double-bond rotation. *J. Phys. Chem. A* **2002**, *106*, 3614–3620.
- 20 Hsieh, C.-C.; Chen, K.-Y.; Chou, P.-T., unpublished results.
- 21 Yu, W.-S.; Cheng, C.-C.; Cheng, Y.-M.; Wu, P.-C.; Song, Y.-H.; Chi, Y.; Chou, P.-T. Excited-state intramolecular proton transfer in five-membered hydrogen-bonding systems: 2-Pyridyl pyrazoles. *J. Am. Chem. Soc.* **2003**, *125*, 10800–10801.
- 22 Waluk, J. Hydrogen-bonding-induced phenomena in bifunctional heteroazaaromatics. *Acc. Chem. Res.* **2003**, *36*, 832–838.
- 23 Kwon, O. H.; Zewail, A. H. Double proton transfer dynamics of model DNA base pairs in the condensed phase. *Proc. Natl. Acad. Sci. U.S.A.* **2007**, *104*, 8703–8708.
- 24 Takeuchi, S.; Tahara, T. The answer to concerted versus step-wise controversy for the double proton transfer mechanism of 7-azaindole dimer in solution. *Proc. Natl. Acad. Sci. U.S.A.* **2007**, *104*, 5285–5290.
- 25 Négrerie, M.; Gai, F.; Bellefeuille, S. M.; Petrich, J. W. Photophysics of a novel optical probe: 7-Azaindole. *J. Phys. Chem.* **1991**, *95*, 8663–8670.
- 26 Chou, P.-T.; Yu, W.-S.; Wei, C.-Y.; Cheng, Y.-M.; Yang, C.-Y. Water-catalyzed excited-state double proton transfer in 3-cyano-7-azaindole: The resolution of the proton-transfer mechanism for 7-azaindoles in pure water. *J. Am. Chem. Soc.* **2001**, *123*, 3599–3600.
- 27 Hsieh, C.-C.; Chen, K.-Y.; Hsieh, W.-T.; Lai, C.-H.; Shen, J.-Y.; Jiang, C.-M.; Duan, H.-S.; Chou, P.-T. Cyano analogues of 7-azaindole: Probing excited-state charge-coupled proton transfer reactions in protic solvents. *ChemPhysChem* **2008**, *9*, 2221–2229.
- 28 Mente, S.; Maroncelli, M. Solvation and the excited-state tautomerization of 7-azaindole and 1-azacarbazole: Computer simulations in water and alcohol solvents. *J. Phys. Chem. A* **1998**, *102*, 3860–3876.
- 29 Nibbering, E. T. J.; Elsaesser, T. Ultrafast vibrational dynamics of hydrogen bonds in the condensed phase. *Chem. Rev.* **2004**, *104*, 1887–1914.